

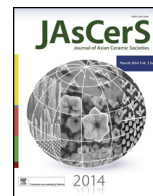
HOSTED BY



Contents lists available at ScienceDirect

Journal of Asian Ceramic Societies

journal homepage: [www.elsevier.com/locate/jascer](http://www.elsevier.com/locate/jascer)



# Bioactivity studies of calcium magnesium silicate prepared from eggshell waste by sol–gel combustion synthesis

Rajan Choudhary, Sivasankar Koppala, Sasikumar Swamiappan\*

Materials Chemistry Division, School of Advanced Sciences, VIT University, Vellore 632014, Tamilnadu, India

## ARTICLE INFO

### Article history:

Received 17 November 2014  
Received in revised form 19 January 2015  
Accepted 21 January 2015  
Available online xxx

### Keywords:

Akermanite  
Eggshell  
Bioactivity  
Hydroxyapatite  
Natural bone mimic

## ABSTRACT

The present study focused on the synthesis of calcium magnesium silicate (akermanite,  $\text{Ca}_2\text{MgSi}_2\text{O}_7$ ) using eggshell biowaste (as calcium source), magnesium nitrate and tetraethyl orthosilicate (TEOS) as starting materials. Sol–gel combustion method was adopted to obtain calcium magnesium silicate. Citric acid was used as a fuel (reducing agent) and nitrate ions present in the metal nitrates acts as an oxidizing agent during combustion process. The characterization of synthesized calcium magnesium silicate was carried out by powder X-ray diffraction (XRD), Fourier transform infrared (FTIR) and scanning electron microscopy (SEM) techniques. Calcium magnesium silicate crystallite size was observed in nano regime which can effectively mimic natural bone apatite composition. In-vitro bioactivity was investigated by immersing calcium magnesium silicate pellet in simulated body fluid (SBF) for three weeks. Results show effective deposition of crystallized hydroxyapatite (HAP) layer on its surface and predicting its possibilities for applications in hard tissue regeneration.

© 2015 The Ceramic Society of Japan and the Korean Ceramic Society. Production and hosting by Elsevier B.V. All rights reserved.

## 1. Introduction

Biosilicates as bone substituents play a vital role in bone tissue engineering. Bone substitution is an advanced therapy for repairing damaged and infected tissues rather than their removal or transplantations. Thus, it minimizes the organ loss and the effect of negative immune response from the human body. Revolution in the replacement of tissue happened with the development of synthetic biomaterials. These can interact with living host tissues and produce certain biological response at the interface of implants. Bone and teeth disorders like osteoporosis and periodontal diseases have drawn attention of the scientists towards the development of bio-ceramics as filler [1]. More importance was given towards using bioactive fixation of implant to tissues by means of forming HAP layer on the implants surface [2].

In mammalian bodies, elements like Ca, Mg and Si play a vital role in bone formation. Calcium is a major content found in bones, teeth and skull, deficiency of which leads to various fatal disorders. Magnesium is required for the regulation of bone growth, repair and maintenance while silicon is the necessary element for skeletal development, and its deficiency can cause skull deformation

[3,4]. Biomaterials containing Ca, Mg, and Si have low degradation rate, significantly improved mechanical strength as compared to conventional biomaterials such as calcium phosphates (HAP) and calcium silicates ( $\text{CaSiO}_3$ ) [5]. Akermanite ( $\text{Ca}_2\text{MgSi}_2\text{O}_7$ ) belongs to sorosilicates class having chemical formula  $\text{X}_2\text{YZ}_2\text{O}_7$ . Previously, akermanite has been prepared by conventional methods such as combustion [6], sintering and crystallization [7], sol–gel process [8] and container less processing method [9].

Literature reports reveal that in-vitro HAP formation ability of akermanite is due to Si rich layer which accelerates the formation of HAP on its surface and controls the precipitation kinetics of bone like apatite deposition when it was immersed in simulated body fluid [10,11]. Akermanite helps in promoting cell proliferation and osteogenic differentiation when trialled for in-vivo test [12–15]. The major objective of the present work is to chemically synthesize akermanite by sol–gel combustion method using eggshell waste as calcium source and evaluation of its in-vitro bioactivity for bone regeneration and dental applications.

## 2. Experimental procedure

### 2.1. Materials

Chicken eggshells, magnesium nitrate (LR, 99.0%, SDFCL), citric acid anhydrous (LR, 99.0%, SDFCL), tetraethyl orthosilicate (98%, Acros Organics), concentrated nitric acid (LR, 69–72%, SDFCL),

\* Corresponding author. Tel.: +91 416 2202464; fax: +91 416 2243092.

E-mail address: [ssasikumar@vit.ac.in](mailto:ssasikumar@vit.ac.in) (S. Swamiappan).

Peer review under responsibility of The Ceramic Society of Japan and the Korean Ceramic Society.

<http://dx.doi.org/10.1016/j.jascer.2015.01.002>

2187-0764 © 2015 The Ceramic Society of Japan and the Korean Ceramic Society. Production and hosting by Elsevier B.V. All rights reserved.

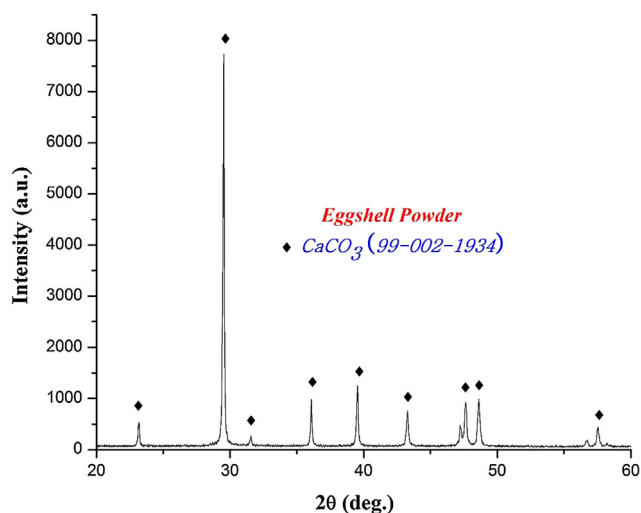


Fig. 1. XRD pattern of crushed eggshell powder.

ethylene diamine tetra acetic acid (LR, 98.0%, SDFCL), Eriochrome Black-T (AR, 99%, SDFCL), ammonia solution (AR, 25%, SRL), ammonium chloride (GR, 98.8%, Merck), sodium chloride (AR, 99.9%, SDFCL), sodium bicarbonate (AR, 99%, Nice Chemicals), potassium chloride (AR, 99.5%, SDFCL), di-potassium hydrogen orthophosphate (AR, 99.0%, SDFCL), magnesium chloride (AR, 99.0%, SDFCL), concentrated hydrochloric acid (LR, 35–38%, SDFCL), calcium chloride (AR, 98%, Qualigen Fine Chemicals), sodium sulphate anhydrous (AR, 99.5%, SDFCL) and tris(hydroxymethyl)aminomethane (AR, 99.8%, SDFCL) were used in the present study.

## 2.2. Extraction of calcium from eggshell waste

Hen eggshells were collected and boiled at 90–100 °C to remove the unwanted protein coatings and microorganism from the shell. The boiled eggshells were dried in a hot air oven for 2 h at 120 °C and then crushed to fine powder by using mortar and pestle. XRD pattern and FTIR spectrum (Figs. 1 and 2) confirm the existence of calcium carbonate as major constituent in eggshell powders [16,17]. Eggshell solution was prepared by dissolving 20 g of fine eggshell powder in 25 ml of nitric acid.

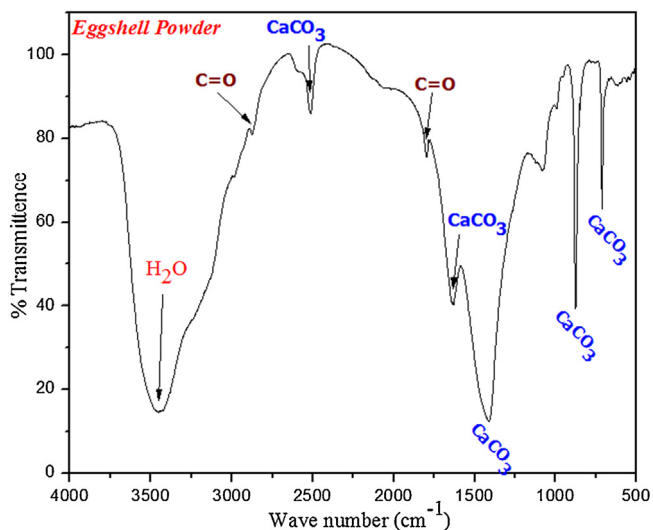


Fig. 2. FTIR spectrum of crushed eggshell powder.

## 2.3. Estimation of calcium ( $\text{Ca}^{2+}$ ) ions by EDTA titration

The concentration of calcium ions ( $\text{Ca}^{2+}$ ) present in the eggshell solution was found to be 1.99 M. It was estimated by EDTA titration as per previous reports [16].

## 2.4. Synthesis of calcium magnesium silicate

(1 M) magnesium nitrate and (3 M) citric acid stock solutions were prepared in deionized water. 20 ml of eggshell solution, 20 ml of magnesium nitrate and 30 ml of citric acid were pipetted out from the stock solution and 9 ml of TEOS was mixed sequentially in a beaker. The pH of the reaction mixture was adjusted to 1 by using concentrated nitric acid. Finally, the reaction mixture was kept for stirring at room temperature for 28 h. Nitric acid plays dual role in sol-gel combustion method by maintaining the pH of the reaction mixture at 1 and also facilitates hydrolysis of TEOS into silanol and ethyl alcohol. The resultant silanol and ethyl alcohol undergoes poly-condensation reaction with the citric acid, leading to the formation of a gel-like complex. The complex was later kept for ageing for 2 days to obtain dense gel. The gel formed was dried at 150 °C for 3 h in hot air oven and eventually decomposed at 400 °C in a preheated muffle furnace for combustion. Combustion initiates with exothermic redox reaction between fuel and nitrate ions present in gel. The production of enormous heat increases the internal temperature of the reaction mixture and achieves the phase formation [6]. Brown colour precursor formed after combustion indicates the existence of nitrate and carbon groups. The precursor was finely powdered by using mortar pestle and calcined at different temperatures for 6 h.

Phase identification of the synthesized akermanite was analyzed by XRD (Bruker, D8 advance, Germany), using  $\text{Cu K}\alpha$ , Ni filtered radiation ( $\lambda = 1.5406 \text{ \AA}$ ). Functional groups present in the samples were examined by FT-IR spectrophotometer (IR Affinity-1, Shimadzu). SEM images were recorded using Hitachi S-3400N Model, at an accelerating voltage of 20 kV.

## 2.5. In-vitro bioactivity studies

The SBF solution was prepared as per Kokubo procedure, since it contains ionic concentration similar to human plasma [18–21]. Synthesized calcium magnesium silicate was thoroughly ground by using mortar and pestle and made into a pellet (12 mm diameter) using hydraulic press. The pellet is then immersed in SBF solution and incubated at 37 °C for three weeks in order to examine HAP deposition on immersed pellet. After every 7th day, the pellet was removed from SBF and washed with the double distilled water and dried for characterization.

## 3. Results and discussion

### 3.1. Characterization

#### 3.1.1. Powder-XRD

XRD pattern (Fig. 3) of the precursor calcined at 900 °C shows the presence of akermanite as the major phase, and merwinite ( $\text{Ca}_3\text{MgSi}_2\text{O}_8$ ) and diopside ( $\text{CaMgSi}_2\text{O}_6$ ) as the secondary phases. With the increase in calcination temperature diopside phase completely disappeared and the intensity of merwinite peaks got reduced. However, at high temperature (1200 °C) akermanite exists as major phase (90%) while merwinite (10%) exists as minor phase. Akermanite phase (Fig. 4) matches with the standard JCPDS pattern (96-900-6937) and indexed to the same. It exists in tetragonal crystal system with the lattice parameter of  $a = 7.83650 \text{ \AA}$  and  $c = 5.01079 \text{ \AA}$ . The crystallite size ( $D$ ) of akermanite was

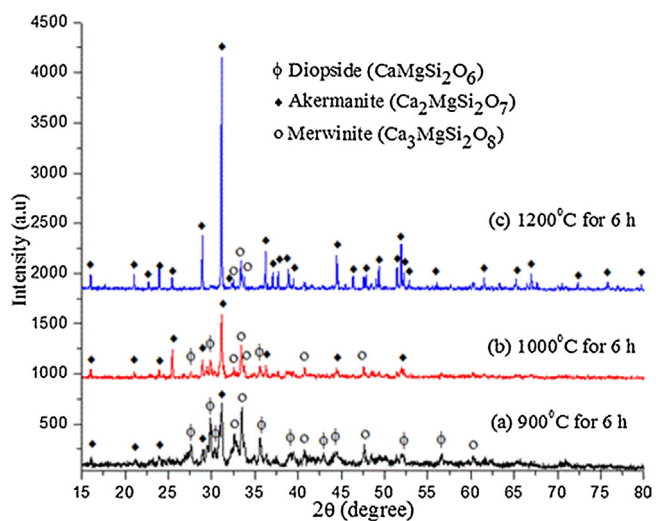


Fig. 3. XRD pattern of calcium magnesium silicate powders at different calcination temperatures.

calculated from the full width at half-maximum (FWHM) values using Scherrer's equation [22].

$$D = \frac{\kappa\lambda}{\beta \cos \theta}$$

where  $\lambda$  is the wavelength of the X-ray,  $\theta$  is the Bragg angle, and  $\kappa$  is the constant. The calculated average crystallite size of akermanite is found in the range of 80–90 nm.

3.1.2. FTIR spectroscopy

FTIR spectra (Fig. 5) of akermanite samples calcined at 1200°C show O–Ca–O bending modes at 415 cm<sup>-1</sup> and O–Mg–O bending modes at 486 cm<sup>-1</sup>. Peak at 586 cm<sup>-1</sup> shows the presence of Ca=O group and the O–Si–O peaks were observed at 640 cm<sup>-1</sup> and 682 cm<sup>-1</sup>. Peaks at 852 cm<sup>-1</sup>, 935 cm<sup>-1</sup> and 974 cm<sup>-1</sup> indicate the Si–O stretching modes. Symmetric stretching at 1024 cm<sup>-1</sup> was assigned to Si–O–Si vibration and asymmetric stretching at 1400 cm<sup>-1</sup> is due to the dissolution of carbon dioxide in silicate bioceramics and results in the formation of distorted carbonate group

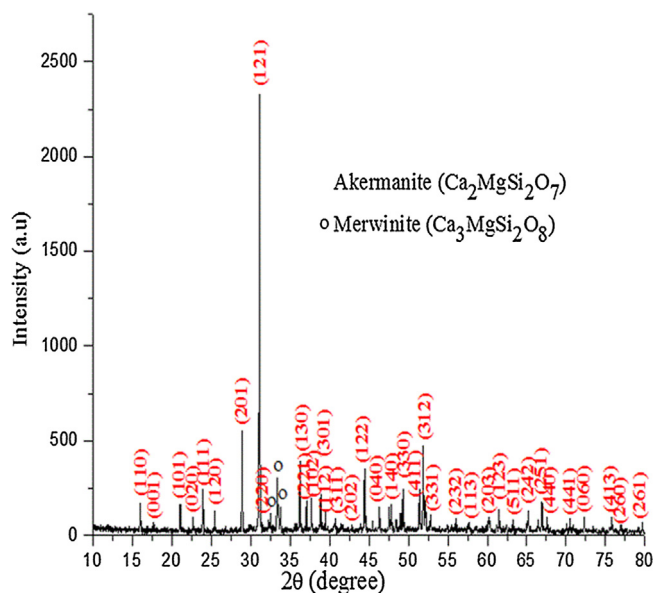


Fig. 4. Indexed XRD pattern of calcium magnesium silicate powders calcined at 1200°C for 6 h.

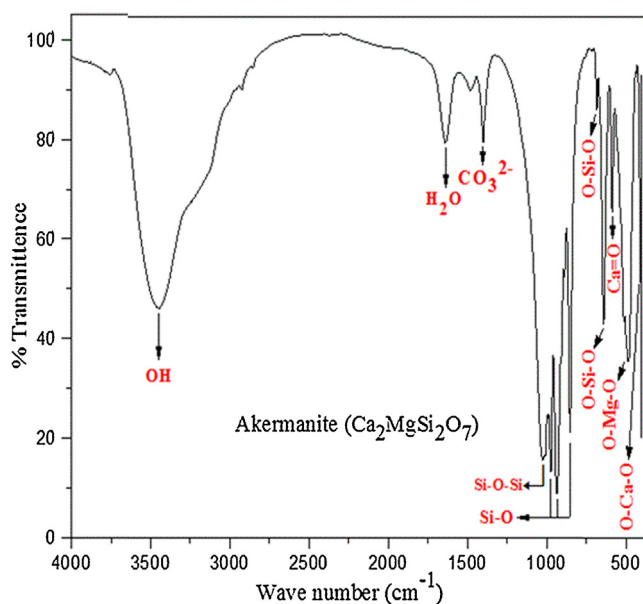


Fig. 5. FTIR spectrum of calcium magnesium silicate powders calcined at 1200°C for 6 h.

causing splitting of IR band. The absorbed carbon dioxide might be from the environment during the reaction process [23]. Bending vibration of H<sub>2</sub>O was observed at 1637 cm<sup>-1</sup> and broad moisture absorption band was observed at 3439 cm<sup>-1</sup> [24–26].

3.2. In-vitro bioactivity studies

Bioactivity of the silicate bioceramics is due to the strong bonding between bioactive glass and the bone mineral which is facilitated by the silica rich layer on the glass surface. When biosilicates are exposed to aqueous physiological environment (SBF) to investigate its in-vitro bioactivity, both chemical composition and structural changes occur on the surface as a function of time factor. During dissolution, cations of the surface get exchanged with H<sup>+</sup>

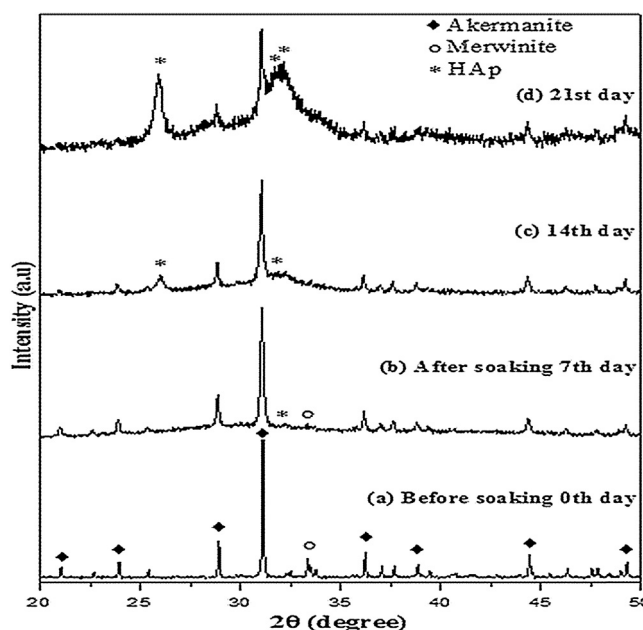


Fig. 6. XRD patterns of calcium magnesium silicate pellet soaked in SBF solution: (a) 0 day, (b) 7 days, (c) 14 days and (d) 21 days.

present in the solution which leads to increase in hydroxyl concentration in the solution and further it reacts with the silica present in the biosilicate network. As a result, the hydrolysis of silica occurs with breakage of Si–O–Si bonds leading to the formation of silanol (Si–OH) in the surface layer and increases the pH of the SBF. The silanol group induces nucleation of HAP by consuming calcium and phosphate ions from the SBF leading to the formation of apatite layer as an interface between the implanted silicate material and bone tissue. The immersing time and circulation of SBF play a major role in the bioactivity of bioceramics [27–29].

### 3.3. Analysis of bone-like apatite formation

#### 3.3.1. XRD analysis

Surface composition of calcium magnesium silicate pellet immersed in SBF was examined by the XRD patterns (Fig. 6) after 7, 14 and 21 days to analyze the deposition of HAP. After 7 days the XRD pattern indicates poor deposition of HAP. The merwinite peaks started becoming less intense which indicates that the dissolution of merwinite happens first and it undergoes hydrolysis. Thus, it helps in deposition of HAP. After 14 days, the immersed surface is partially covered by HAP layer whereas merwinite peaks totally disappear in the XRD pattern. When the surface was analyzed after 21 days, an intense HAP layer was observed in the XRD pattern which shows that there is an increase in the crystallization of HAP layer with increase in immersing time. Previously, it was reported that the formation of HAP layer was observed on pure akermanite after 10 days [8]. These results indicate that the presence of merwinite phase helps in the faster deposition of HAP.

#### 3.3.2. FTIR analysis

The FTIR spectrum (Fig. 7) of calcium magnesium silicate pellets immersed in SBF for in-vitro bioactivity studies shows gradual decrease in relative intensities of some functional groups such as Ca=O, O–Si–O and Si–O whereas O–Ca–O and O–Mg–O peaks have completely disappeared and were replaced by phosphate group which strengthens the argument of hydrolysis of calcium and magnesium taking place in the initial stages of bioactivity studies. After 21 days of bioactivity studies, bending vibration of phosphate groups was noticed at  $478\text{ cm}^{-1}$  and  $563\text{ cm}^{-1}$  while stretching vibration of phosphate group is observed at  $1031\text{ cm}^{-1}$ . These phosphate peaks confirm the mineralization of HAP on the surface of the immersed pellet. The vibration bands at  $1419\text{ cm}^{-1}$  and  $1483\text{ cm}^{-1}$  show the presence of carbonate group. Thus, carbonate group present in the synthesized powder did not undergo any change which indicates that it is not metal carbonates such as  $\text{MgCO}_3$  and  $\text{CaCO}_3$  as they will dissolve in simulated body fluid.

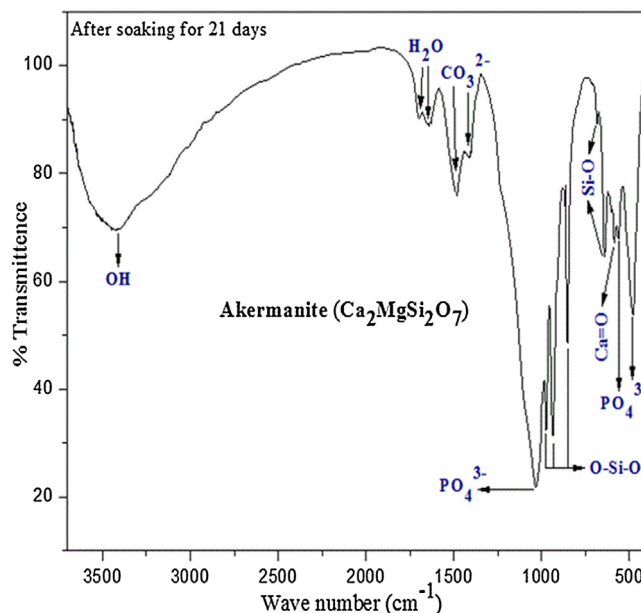


Fig. 7. FTIR spectrum of calcium magnesium silicate pellet soaked in SBF solution for 21 days.

Bending vibration of absorbed  $\text{H}_2\text{O}$  was observed at  $1641\text{ cm}^{-1}$  and  $1697\text{ cm}^{-1}$  whereas stretching vibration of moisture absorption band corresponds to  $3385\text{ cm}^{-1}$  [30–33].

#### 3.3.3. Scanning electron microscopy

SEM was used to characterize the morphological parameters of the synthesized bioceramic in nano to micron scale [34]. The surface characteristics such as surface porosity and morphology of the implants help in regulation of cell proliferation, cell attachment and protein adsorption [35]. SEM images of calcium magnesium silicate before and after bioactivity studies are shown in Fig. 8. SEM image (Fig. 8(A)) of calcined calcium magnesium silicate powders before immersing in SBF solution shows porous surface, agglomerated and irregular surface morphology. Porous nature might be due to release of gases during exothermic combustion reaction. Previously, it has been reported that porosity accelerates ion exchange process between the bioceramic and SBF causing faster dissolution and apatite formation. Interaction between the biomaterial implant and the surrounding tissues is more for porous and agglomerated surface [36–38]. Fig. 8(B) represents SEM image of calcium magnesium silicate pellet after immersion in SBF for 21 days. It reveals that the surface was fully covered by small bubbles with appearance of

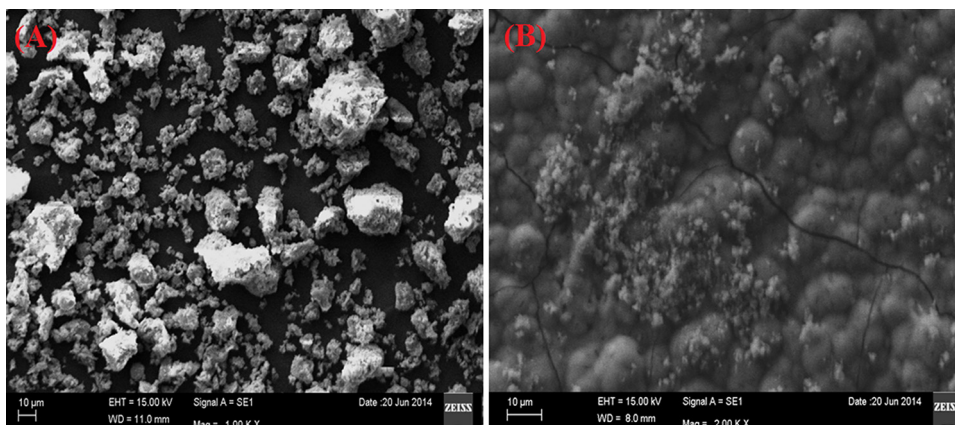


Fig. 8. SEM images. (A) Calcium magnesium silicate powders before SBF immersion. (B) Calcium magnesium silicate pellet after SBF immersion.

minute pores and cracks throughout the surface. Appearance of tiny particles cluster provides an appearance of hydroxyapatite deposition with fur like morphology. These surface properties reveal that calcium magnesium silicate bioceramic enhances the kinetics of biomineralization of hydroxyapatite layer on the implant surface.

#### 4. Conclusion

Calcium magnesium silicate powder was chemically synthesized by sol–gel combustion method. Eggshell was used as a calcium source for the first time to prepare calcium magnesium silicate, which proves a way to convert the biological waste into a valuable bioceramics. Apatite formation starts after 7 days on the surface of calcium magnesium silicate immersed in SBF solution. Rate of apatite deposition was found to increase with increase in immersion period. This study suggests the bioactive nature of calcium magnesium silicate and might be a potential candidate material to use in bone regeneration and dental applications.

#### Acknowledgements

This research was financially supported by Vellore Institute of Technology Research Grants for Engineering, Management and Science (VITRGEMS) and the authors thank DST-FIST for the XRD facility.

#### References

- [1] M.N. Rahaman, D.E. Day, B.S. Bal, Q. Fu, S.B. Jung, L.F. Bonewald and A.P. Tomsia, *Acta Biomater.*, 7, 2355–2373 (2011).
- [2] L.L. Hench, *J. Am. Ceram. Soc.*, 74, (7) 1487–1510 (1991).
- [3] C.C. Liu, J.K. Yeh and J.F. Aloia, *J. Bone Miner. Res.*, 3, S104 (1988).
- [4] E.M. Carlisle, *J. Nutr.*, 110, 1046–1055 (1979).
- [5] C. Wu and J. Chang, *J. Biomed. Mater. Res. Part B*, 153–160 (2007).
- [6] V.B. Bhatkar and N.V. Bhatkar, *Int. J. Adv. Eng. Sci. Technol.*, 5, (2) 184–186 (2011).
- [7] J.M.F. Ferreira, D.U. Tulyaganov, S. Agathopoulos and J.M. Ventura, *Mater. Lett.*, 60, 1488–1491 (2006).
- [8] C. Wu and J. Chang, *Mater. Lett.*, 58, 2415–2417 (2004).
- [9] C. Wu, M. Zhang, D. Zhai, J. Yu, Y. Liu, H. Zhu and J. Chang, *J. Mater. Chem. B*, 1019–1026 (2012).
- [10] C. Wu, J. Chang, S. Ni and J. Wang, *J. Biomed. Mater. Res.*, 76, (A) 73–80 (2006).
- [11] X. Hou, G. Yin, X. Chen, X. Liao, Y. Yao and Z. Huang, *Appl. Surf. Sci.*, 257, 3417–3422 (2011).
- [12] S. Yin, Q. Liu, L. Cen, L. Chen, G. Liu, J. Chang and L. Cui, *Biomaterials*, 29, 4792–4799 (2008).
- [13] H. Suna, C. Wu, K. Dai, J. Chang and T. Tang, *Biomaterials*, 27, 5651–5657 (2006).
- [14] Y. Huang, X. Jin, X. Zhang, H. Sun, J. Tu, T. Tang, J. Chang and K. Dai, *Biomaterials*, 30, 5041–5048 (2009).
- [15] L. Xia, Z. Zhang, L. Chen, W. Zhang, D. Zeng, X. Zhang, J. Chang and X. Jiang, *Eur. Cell Mater.*, 22, 68–83 (2011).
- [16] A. Udduttula and S. Swamiappan, *Bull. Mater. Sci.*, 37, (2) 207–212 (2014).
- [17] G. Krithiga and T.P. Sastry, *Bull. Mater. Sci.*, 34, (1) 177–181 (2011).
- [18] T. Kokubo and H. Takadama, *Biomaterials*, 27, 2907–2915 (2006).
- [19] T. Kokubo, *J. Non Cryst. Solids*, 120, 138–151 (1990).
- [20] J. Ma, C.Z. Chena, D.G. Wang, X. Shao, C.Z. Wang and H.M. Zhang, *Ceram Int.*, 38, 6677–6684 (2012).
- [21] A. Udduttula, S. Koppala and S. Swamiappan, *Trans. Ind. Ceram. Soc.*, 72, (4) 257–260 (2013).
- [22] H. Klug and L. Alexander, *X-ray Diffraction Procedures*, John Wiley and Sons Inc., New York (1962).
- [23] A.M. Kalinkin, V.V. Boldyrev, A.A. Politovaa, E.V. Kalinkina, V.N. Makarov and V.T. Kalinnikov, *Glass Phys. Chem.*, 29, (4) 410–414 (2003).
- [24] K. Omori, *Am. Mineral.*, 56, 1607–1616 (1971).
- [25] B. Engin, H. Demirtas and M. Eken, *Radiat. Phys. Chem.*, 75, 268–277 (2006).
- [26] F.A. Miller and C.H. Wilkins, *Anal. Chem.*, 24, (8) 1253–1294 (1952).
- [27] X. Liu, C. Ding and P.K. Chu, *Biomaterials*, 25, 1755–1761 (2004).
- [28] T. Kokubo, *Acta. Mater.*, 46, 2519–2527 (1998).
- [29] F. Tavangarian and R. Emadi, *Mater. Lett.*, 65, 740–743 (2011).
- [30] S. Sasikumar and R. Vijayaraghavan, *J. Mater. Sci. Technol.*, 26, (12) 1114–1118 (2010).
- [31] D. Yi, C. Wu, X. Ma, H. Ji, X. Zheng and J. Chang, *Biomed. Mater.*, 7, 1–9 (2012).
- [32] L. Berzina-Cimdina and N. Borodajenko, in *Research of Calcium Phosphates Using Fourier Transform Infrared Spectroscopy*, *Infrared Spectroscopy – Materials Science, Engineering and Technology*, Ed. by T. Theophile, (2012), ISBN 978-953-51-0537-4.
- [33] U. Vijayalakshmi and S. Rajeswari, *Trends Biomater. Artif. Organs*, 19, (2) 57–62 (2006).
- [34] L. Froberg and L. Hupa, *Appl. Surf. Sci.*, 254, 1622–1629 (2008).
- [35] S.R. Paital and N.B. Dahotre, *Mater. Sci. Eng. R*, 66, 1–70 (2009).
- [36] E. Saiz, M. Goldman, J.M. Gomez-Vega, A.P. Tomsia, G.W. Marshall and S.J. Marshall, *Biomaterials*, 23, 3749–3756 (2002).
- [37] A. Montenero, G. Gnappi, F. Ferrari, M. Cesari, E. Salvioli, L. Mattogno, S. Kaciulis and M. Fini, *J. Mater. Sci.*, 35, 2791–2797 (2000).
- [38] R. Lakshmi, V. Velmurugan and S. Sasikumar, *Combust. Sci. Technol.*, 185, (12) 1777–1785 (2013).